Am J Cancer Res 2021;11(11):5358-5373
www.ajcr.us /ISSN:2156-6976/ajcr0130546

Original Article

An unprecedented endocrine target for ovarian cancer: inhibiting 17β-HSD7 supresses cancer cell proliferation and arrests G2/M cycle

Ruixuan Wang, Tang Li[#,*], Guangren Li[*], Sheng-Xiang Lin

Axe Molecular Endocrinology and Nephrology, CHU Research Center and Université Laval, 2705 Boulevard Laurier, Sainte-Foy, Québec G1V 4G2, Canada. [#]Present address: Dalian Institute of Chemical Physics, Chinese Academy of Sciences, Dalian 116023, China. [*]Co-second authors.

Received January 21, 2021; Accepted August 13, 2021; Epub November 15, 2021; Published November 30, 2021

Abstract: Epithelial ovarian cancer, widely suggested as endocrine-related cancer, yields a low survival rate among patients. Despite intensive research for nearly a century, there have been no fundamental advances in treatment. The reductive 17β-HSD7 is a special enzyme possessing a remarkable dual activity in both the biosynthesis of the most potent estrogen estradiol and the inactivation of the most active androgen dihydrotestosterone. In the present study, we observed over-expression of 17β-HSD7 in EOC cells such as OVCAR-3 and SKOV-3, in agreement with integrative data analysis demonstrating overexpression of 17β-HSD7 in EOC tissues. After knocking down 17β-HSD7, SKOV-3 cell proliferation decreased by 29%, cell arrest in the G2/M phase increased by 25% with cyclin B1/Cdk1 inhibition. Inhibition of 17β-HSD7 in EOC cells triggered negative feedback of its expression, which further decreased the estradiol level to more than 60% under the experimental condition. Such inhibition increased the dihydrotestosterone level to many times higher and suppressed cell proliferation. Thus, 17β-HSD7 is demonstrated to be a promising target for the endeavor against the malignant ovarian cancer, a menace in human life. The targeting of such an enzyme thus provides exceptional scientific importance.

Keywords: 17β-HSD type 7, estradiol, dihydrotestosterone, G2/M cell-cycle arrest, cyclin B1/Cdk1 complex

Introduction

Ovarian cancer (OC) has a low survival rate among gynecological malignancies [1]. The latest statistics of 2018 showed approximately 22,240 new cases of OC diagnosed and 14,070 OC deaths in America [2]. Approximately 90% of ovarian cancers cases are epithelial [3, 4]. Most patients are asymptomatic until OC has widely metastasized within the abdomen [5]. In general, 70% of epithelial ovarian cancer (EOC) is diagnosed at an advanced stage, leading to a very poor survival rate [3, 6]. The five-year relative survival rate for 2009 to 2015 is only 47.6% (https://seer.cancer.gov/statfacts/html/ovary.html). The primary treatments for OC are surgery and cytotoxic chemotherapy [7]. Recent clinical trials reveal that adjuvant chemotherapy only improved overall survival rate by 8% in early-stage EOC [8]. Adjuvant chemotherapy has been suggested to be of no benefit to patients who have undergone complete debulking and staging [9].

Most women develop EOC during their postmenopause years. Evidence has shown that steroid hormones are associated with ovarian tumorigenesis [5, 10, 11]. It is similar to hormone-responsive cancers such as endometrial, breast, and prostate, in which sex hormone receptors are widely expressed [12]. The estrogen receptor α (ERα) is expressed in 60%-80% of OC, while the androgen receptor (AR) is expressed in up to 90% of OC [11, 13]. Based on epidemiological evidence, steroid hormones (estrogens and androgens) effectively stimulate EOC cells, potentially influencing OC transformation [14]. The therapeutic strategy of targeting hormone receptors is successful in several hormone-responsive cancers such as breast and prostate cancer [15-17]. However, only limited success has been reported in OC [6, 11, 18, 19]. The reason why endocrine therapy has not been significantly used in OC therapy requires further investigation. A lack of detailed mechanistic

studies for EOC, and only a limited number of models to understand *in vitro* and *in vivo* hormone responses were proposed [20]. Thus, unveiling the mechanism of hormone action in EOC will benefit the hormonal therapy.

The reductive 17β-hydroxysteroid dehydrogenases (17β-HSDs) comprise key enzymes involved in the final step of the formation of estradiol (E2), and their intracrinology activities in post-menopausal women have been studied [21, 22]. These enzymes play critical roles in various endocrine-related cancers [23]. Reductive 17β-HSD types 1 and 7 are the most important members of the reductive 17β-HSDs and have been studied extensively in hormone-dependent breast cancer (BC) [16, 17, 24]. In comparison to normal ovarian tissues, the increased E2/E1 ratio and higher levels of reductive 17β-HSD mRNAs indicate the potential pivotal roles of these enzymes in EOC [25]. 17β-HSD7 has a critical role in E2 formation and was found to be able to convert dihydrotestosterone (DHT) into 5R-androstane-3β, 17β-diol (3β-diol) [16]. Therefore, it plays a role in modulating mitogenic estrogen and androgen levels in humans. 17β-HSD1 has a critical role in the regulation of E2.

To identify major targets for EOC endocrine treatment, we focused on the study of sex-hormone activation and inactivation via reductive 17β-HSDs in EOC. In the present study, we performed an extensive verification of their expression in EOC and evaluated the biological function of these enzymes in EOC cells. The identification of reductive 17β-HSD7 as an EOC target may open a new pathway for treating this malignancy.

Material and methods

Integrative analysis of clinical datasets

The mRNA expression microarray database was extracted from five ovarian cohorts through the Oncomine database (https://www.oncomine.org). It included gene expression data for 958 ovarian serous cystadenocarcinoma (the primary subtype of EOC) samples [3], as well as 37 normal ovary tissues for reference. The datasets were analyzed for the expression of HSD17B7 in tumor tissue vs. normal tissue. Data analysis was performed with the Meta-analysis to determine the differential expression of HSD17B7 between tumor and normal tissues. The Meta-Analyses was performed in R with the metafor Package.

Cell culture

The EOC cell line OVCAR-3 was grown in culture medium RPMI-1640 medium (Gibco, Life Technologies, Paisley, Scotland), supplemented with 20% fetal bovine serum (FBS) (Sigma, Oakville, ON, Canada). RPMI-1640 medium containing 20% dextran-coated charcoal- (Sigma, St. Louis, MI, USA) stripped FBS was used as hormone-free (HF) culture medium. The EOC cell line SKOV-3 cells were grown in McCoy's 5A culture medium (GE Healthcare, QC, Canada), supplemented with 10% FBS. McCoy's 5A containing 10% dextran-coated charcoal stripped FBS was used as an HF culture medium. Human ovarian surface epithelial cells HOSEpiC was purchased from ScienCell Research Laboratories (San Diego, CA, USA). HOSEpiC culture used the Ovarian epithelial cell medium (ScienCell, San Diego, CA, USA). The three cell lines were grown in a 5% CO_2 atmosphere at 37°C.

Chemical and biological characteristics of inhibitors

The inhibitors of 17β-HSD1 and 17β-HSD7, respectively INH1(18) [26] and INH7(81) [27] were chemically synthesized and biologically selected (**Table 1**) originally by Dr. Donald Poirier. The inhibitors were dissolved in dimethyl sulfoxide (DMSO) as stock solutions and were diluted to final concentrations with HF medium.

siRNA synthesis and transfections

Sense and antisense sequences of target protein siRNAs (Supplementary Table 1) were synthesized and purified by HPLC by Gene Pharma (Shanghai, China). According to the manufacturer's instructions, the 100 nM mixed duplex siRNAs were transfected into cells by Lipofectamine 2000 (Invitrogen, Burlington, ON, Canada). Control cells were transfected with control siRNA provided by Gene Pharma (Shanghai, China) as a negative control (Supplementary Table 1).

Quantitative real-time PCR

Total RNA was extracted from EOC cells by the RNeasy Plus mini kit (Qiagen, Hilden, DE) and

Table 1. Characteristics of 17β-HSD1 and 17β-HSD7 inhibitors

Inhibitor	Chemical structure	IC_{50} E1 to E2	Inhibition (%) DHT to 3β-diol
17β-HSD1 inhibitor INH1(18) [29]	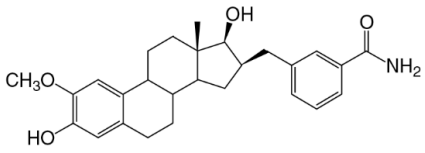	275±5 nM [29]	
17β-HSD7 inhibitor INH7(81) [30]	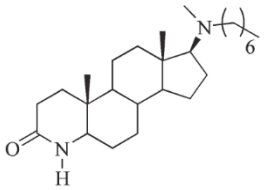	458±38 nM [30]	29% (0.3 μM) 74% (3 μM)

IC_{50}: concentration of the inhibitors inhibiting 50% of E1 to E2 transformation in T47D cells or HEK293 cells overexpressed 17β-HSD7. Inhibition (100%): Inhibition (%) of DHT to 3β-diol conversion in HEK293 cells overexpressed 17β-HSD7. None: Data not shown.

the first-strand cDNA was synthesized using the SuperScript® III First-Strand Synthesis System (Invitrogen, ON, Canada). Thirty nanograms of total cDNA for each sample was subjected to a quantitative real-time polymerase chain reaction (qRT-PCR) using the Fast Start Essential DNA Green Master (Roche Diagnosis, Mannheim, DE). Reactions were performed in triplicate with a final primer concentration of 0.5 μM. The housekeeping gene 18s was used as a reference. The primers used for 18s were: 5'-ACG GAC CAG AGC GAA AGC ATT-3' and 5'-TCC GTC AAT TCC TTT AAG TTT CAG CT-3'; 17β-HSD1: 5'-CTT CTT TGT CCC CTG GGT CTG TGT G-3' and 5'-GTC TCA CTG TGT TGC TCT GGC TGG T-3'; 17β-HSD7: 5'-TCC ACC AAA AGC CTG AAT CTC TC-3' and 5'-GGG CTC ACT ATG TTT CTC AGG C-3'. The manufacturer's protocol for the Fast Start Essential DNA Green Master was followed for qRT-PCR. A LightCycler® 96 Real-Time PCR System (Roche Diagnosis, Mannheim, DE) was used. Several qRT-PCR reactions were tested by Plateforme de Séquençage et de Génotypage des Génomes (QC, Canada) and subjected to DNA sequencing to confirm the specificity of the reactions. The LightCycler Software supplied by the manufacturer was used to calculate data and create a specific standard curve for each 17β-HSD mRNA. The mRNA levels were expressed as mRNA copies/mg total RNA, and SDs were <10% of triplicates. All the primers were designed using online software Primer 3 web version 4.0.0 (http://primer3.ut.ee/) and synthesized by Integrated DNA Technologies (IA, USA).

Cell proliferation assay

Cell proliferation changes were measured by CyQuant cell proliferation kit (Molecular Probes, Invitrogen, ON, Canada). The kit determines cell numbers by staining nucleic acids (DNA and RNA). The EOC cells were plated at a density of 3×10^3 cells per well in 96-well plates. Dehydroepiandrosterone (DHEA) and E1 (Sigma, St. Louis, MI, USA) were used as substrates. The cell culture medium was changed every 48 h. The cells were washed twice with 1×PBS and frozen for more than 24 h at -80°C. Two hundred microliters of CyQuant GR dye/cell-lysis buffer were added to each well after the plates were thawed at room temperature for 15 min. Fluorescence data were measured using a fluorescence microplate reader at 489 nm excitation and 520 nm emission. Quadruplicate wells were used for each condition and repeated in three independent experiments.

Cell cycle analysis

EOC cells were plated at a density of 6×10^4 cells per well in 6-well plates. Cells were treated with siRNA at their protocol concentrations with E1 or DHEA as substrates for 96 hours. The medium was half-changed every 48 hours. The cells were fixed with 70% ethanol and stained with DAPI/Triton X-100 solution (Sigma, St. Louis, MI, USA) before analysis by flow cytometry using the BD LSR II (BD Bioscience). The results are shown as the percentage of total cells in the G0/G1, S, and G2/M phases.

Duplicate wells were used for each condition and repeated in three independent experiments.

Protein extraction and western blot

The EOC cells were treated with specific siRNAs for 96 hours. Total proteins from cells were extracted by RIPA buffer (Invitrogen, Burlington, ON, Canada) with 1% protease inhibitor cocktail (EMD Chemicals, Gibbstown, NJ, 100:1 v/v). Fifty micrograms of total cell protein were separated on a 12% SDS-PAG, then electroblotted onto polyvinylidene difluoride (PVDF) membranes (Amersham Hybond-PTM, GE Healthcare, QC, Canada). The primary antibodies used were anti-17β-HSD1 (SAB1403946) (Sigma, St. Louis, MI, USA) 1:500, anti-17β-HSD7 (ab112006) (Abcam, Cambridge, MA, USA) 1:500, anti-cyclin B1 (ab32053) (Abcam, Cambridge, MA, USA) 1:10000, anti-cyclin dependent kinase 1 (Cdk1) (ab133327) (Abcam, Cambridge, MA, USA) 1:10000 and anti-β-actin (ab3289) (Abcam, Cambridge, MA, USA) 1:5000. The anti-β-actin antibody was used as a loading control. The goat-anti-rabbit IgG-HRP (sc-2004) 1:5000 and goat-anti-mouse IgG-HRP (sc-2005) (Santa Cruz Biotechnology, CA, USA) 1:2000 were used as secondary antibodies. Blots were visualized with Western Lighting Plus ECL (PerkinElmer, MA, USA) enhanced chemiluminescence substrate for western blotting, followed by exposure to X-ray films. The target band densities were quantified using the Image program (Molecular Dynamics, Sunnyvale, CA). All samples were tested in triplicate and repeated in three independent experiments. The ratios between the target protein and corresponding β-actin were calculated to determine the relative protein expression. Calculation of the Percentage (%) change and the coefficient of variation (CV) was based on:

$$\%\ \text{change} = \left(\frac{\textit{normalized signal SAMPLE}}{\textit{normalized signal CONTROL}} - 1\right) \times 100\%$$

$$\text{CV} = \frac{\textit{standard deviation of fold change for replicates}}{\textit{mean fold change of replicates}} \times 100\%$$

E2 and DHT concentration

EOC cells were plated in 96-well plates at the same density of cell proliferation assay and treated with siRNA or inhibitors with the substrates E1 (0.1 nM), DHEA (100 nM) or DHEA (1 μM). We determined the E2 and DHT levels in the culture supernatants were immediately with the Estradiol EIA Kit (Cayman Chemical, Ann Arbor, MI, USA) and DHT ELISA Kit (Alpha Diagnostic International, San Antonio, TX, USA). According to the manufacturer's instructions, we prepared duplicate wells for each sample. The sample's absorbance was measured at 412 nM for E2 ELISA analysis and 450 nM for DHT ELIAS. Data were reported as picomolar (pM). Each condition was tested in duplicate, and experiments were repeated three times.

Statistical analysis

All results were calculated using Microsoft Excel 2010. The unpaired, two-sided Student test was used to compare two groups. The statistical difference was considered significant when $P \leq 0.05$ and regarded as highly significant when $P \leq 0.001$. The Meta-Analyses of Oncomine mRNA expression microarray database calculated in R.

Results

Elevated expression of reductive 17β-HSD7 in EOC tissue compared with normal ovary tissue

We found significant up-regulation of 17β-HSD7 in ovarian carcinoma tissues (**Figure 1A** and **1B**) in the integrative analysis. The *P*-value is <0.01, I^2=94% and τ^2=0.9536. The 95% CI in the Fixed effect model is 0.76 to 1.11, and the 95% CI in the Random-effects model is -0.14 to 1.69. We confirmed the relative expression of 17β-HSD7 between EOC cell lines and human ovarian surface epithelial cells HOSEpiC (**Figure 1C**). There is 22% (CV: 9%) up-regulation in SKOV-3, but there is 31% (CV: 4%) down-regulation in OVCAR-3.

Reductive 17β-HSD messenger RNA levels in epithelial ovarian cancer cells

Both 17β-HSDs type 7 and type 1 mRNAs are expressed in EOC cell lines as determined by qRT-PCR analysis. However, the major difference was that the 17β-HSD7 copy number being around half of 17β-HSD1 number in OVCAR-3 (**Table 2**). This comparison was reversed in SKOV-3. The 17β-HSD7 mRNA level

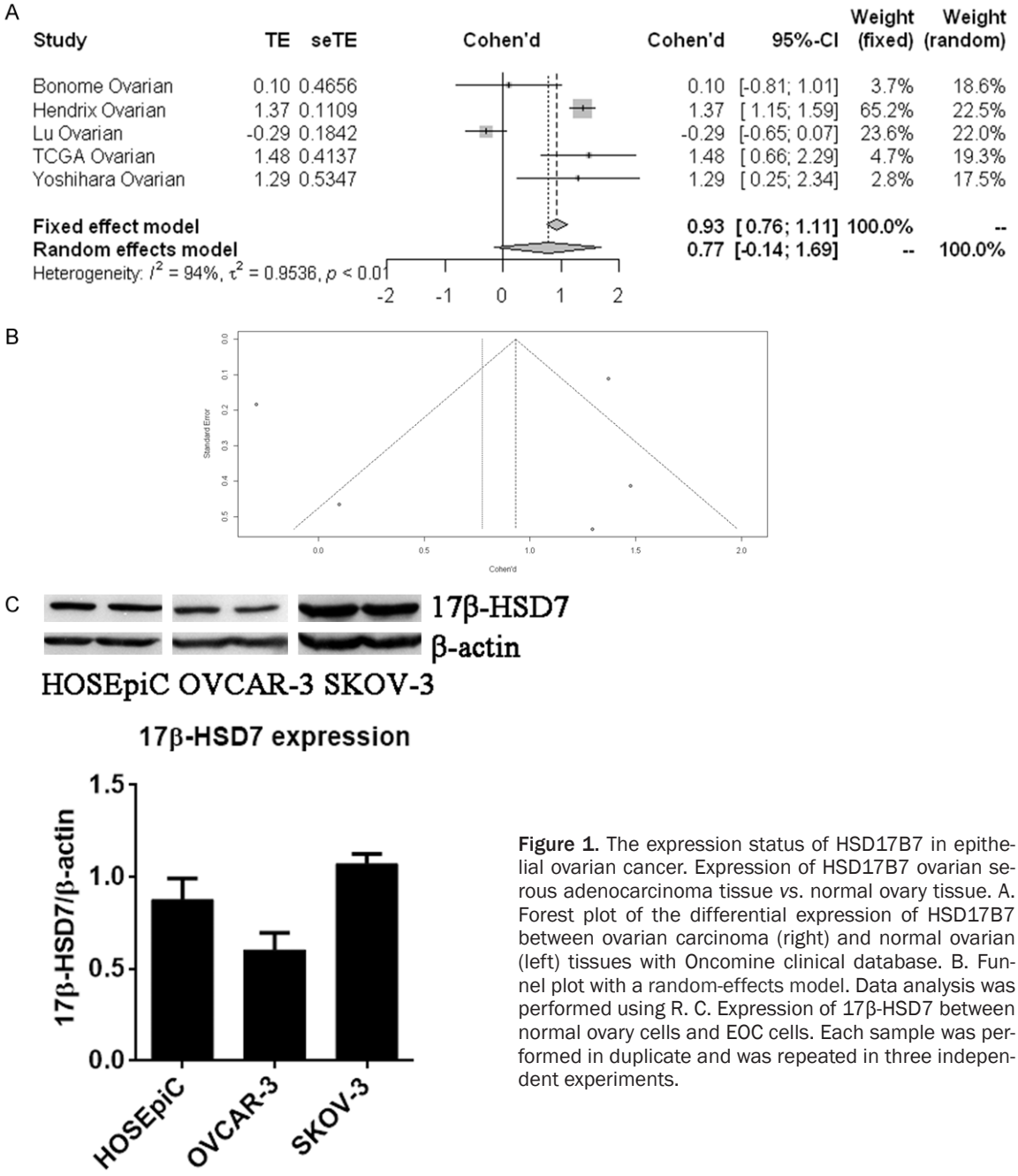

Figure 1. The expression status of HSD17B7 in epithelial ovarian cancer. Expression of HSD17B7 ovarian serous adenocarcinoma tissue *vs.* normal ovary tissue. A. Forest plot of the differential expression of HSD17B7 between ovarian carcinoma (right) and normal ovarian (left) tissues with Oncomine clinical database. B. Funnel plot with a random-effects model. Data analysis was performed using R. C. Expression of 17β-HSD7 between normal ovary cells and EOC cells. Each sample was performed in duplicate and was repeated in three independent experiments.

Table 2. Expression of 17β-HSDs in EOC cells

17β-HSDs	mRNA copies number/mg total RNA	
	OVCAR-3	SKOV-3
17β-HSD1	1.79E+07±2.34E+05	7.15E+06±1.09E+05
17β-HSD7	7.56E+06±7.52E+05	1.73E+07±8.37±05

was 2.4-fold that of 17β-HSD1 in SKOV-3 (**Table 2**). These results show that 17β-HSD type 7 and type 1 are differentially expressed in the two cell lines.

17β-HSD7 knockdown decreased cell growth and arrested cell cycle in the G2/M phase by inhibiting the cyclin B1/Cdk1 complex

17β-HSD7 expression was silenced 86% vs. control by 100 nM mixed specific siRNAs in OVCAR-3 cells as analyzed by qRT-PCR 72 hours after transfection (**Figure 2A**). The specific siRNAs silenced approximately 75% of 17β-HSD1 expression (**Figure 4A**).

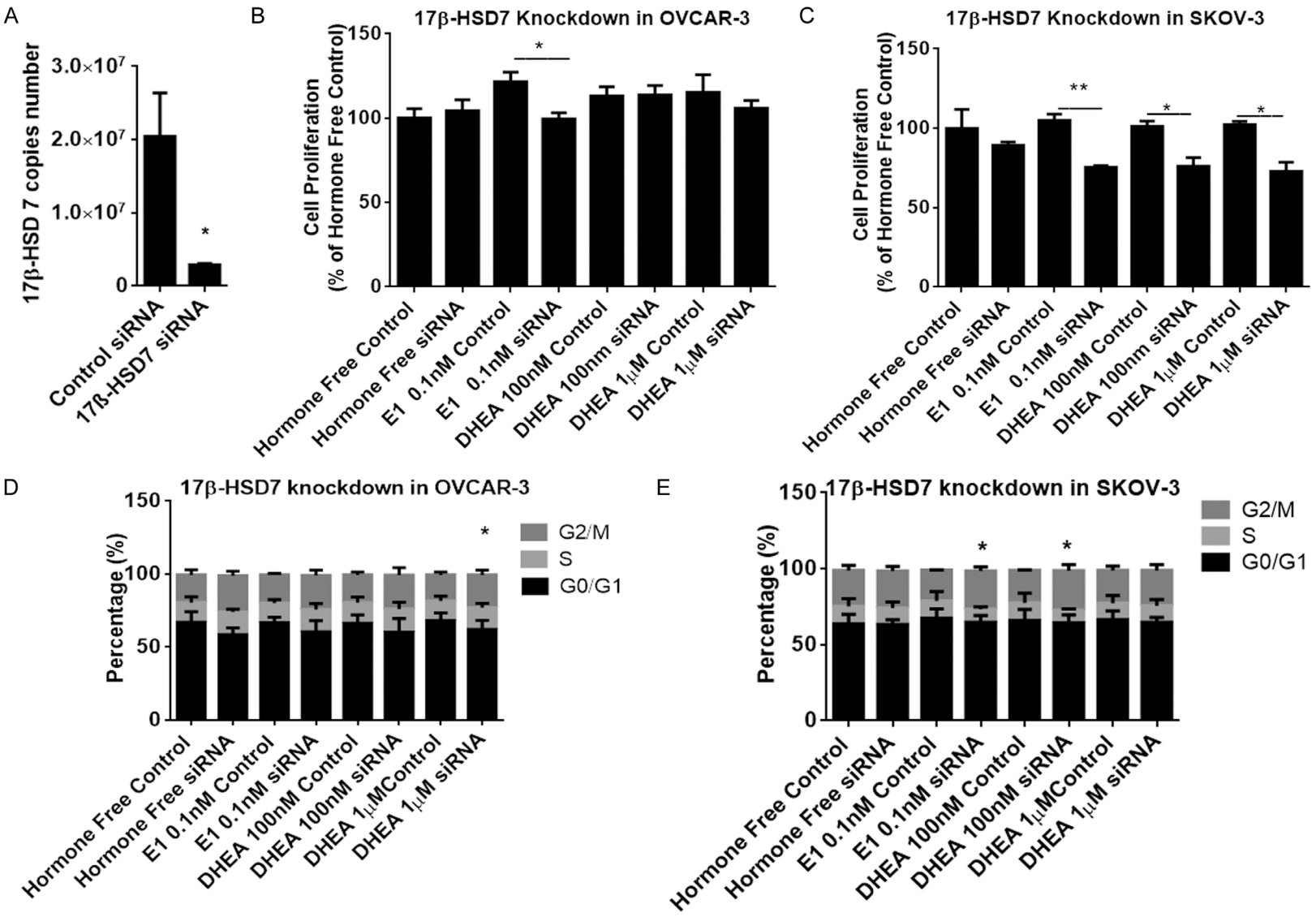
A
17β-HSD 7 copies number
3.0×10^7
2.0×10^7
1.0×10^7
0
*
Control siRNA
17β-HSD7 siRNA
B
17β-HSD7 Knockdown in OVCAR-3
Cell Proliferation (% of Hormone Free Control)
150
100
50
0
*
Hormone Free Control
Hormone Free siRNA
E1 0.1nM Control
E1 0.1nM siRNA
DHEA 100nM Control
DHEA 100nm siRNA
DHEA 1μM Control
DHEA 1μM siRNA
C
17β-HSD7 Knockdown in SKOV-3
Cell Proliferation (% of Hormone Free Control)
150
100
50
0
**
*
*
Hormone Free Control
Hormone Free siRNA
E1 0.1nM Control
E1 0.1nM siRNA
DHEA 100nM Control
DHEA 100nm siRNA
DHEA 1μM Control
DHEA 1μM siRNA
D
17β-HSD7 knockdown in OVCAR-3
Percentage (%)
150
100
50
0
*
G2/M
S
G0/G1
Hormone Free Control
Hormone Free siRNA
E1 0.1nM Control
E1 0.1nM siRNA
DHEA 100nM Control
DHEA 100nM siRNA
DHEA 1μMControl
DHEA 1μM siRNA
E
17β-HSD7 knockdown in SKOV-3
Percentage (%)
150
100
50
0
*
*
G2/M
S
G0/G1
Hormone Free Control
Hormone Free siRNA
E1 0.1nM Control
E1 0.1nM siRNA
DHEA 100nM Control
DHEA 100nM siRNA
DHEA 1μMControl
DHEA 1μM siRNA

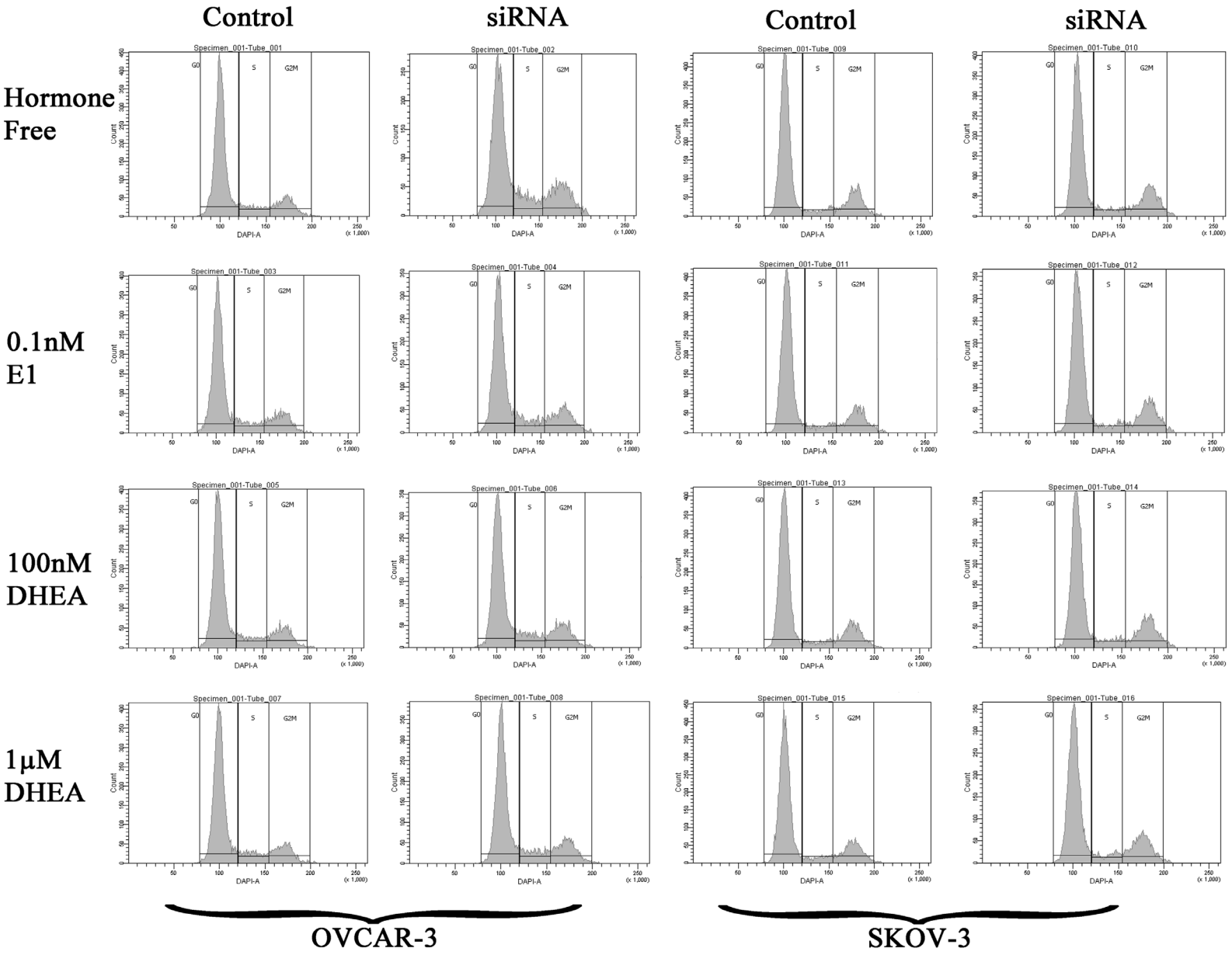
Control
siRNA
Control
siRNA
Hormone Free
0.1nM E1
100nM DHEA
1μM DHEA
Specimen_001-Tube_001
Specimen_001-Tube_002
Specimen_001-Tube_009
Specimen_001-Tube_010
Specimen_001-Tube_003
Specimen_001-Tube_004
Specimen_001-Tube_011
Specimen_001-Tube_012
Specimen_001-Tube_005
Specimen_001-Tube_006
Specimen_001-Tube_013
Specimen_001-Tube_014
Specimen_001-Tube_007
Specimen_001-Tube_008
Specimen_001-Tube_015
Specimen_001-Tube_016
G0
S
G2M
Count
DAPI-A
(x 1,000)
OVCAR-3
SKOV-3

Figure 2. Cell proliferation and cell cycle analysis after 17β-HSD7 siRNA transfection 96 h in EOC cells. 100 nM mixed 17β-HSD7 specific siRNA and control siRNA were used. Different hormone sources were provided: E1 (0.1 nM) and DHEA (100 nm and 1 μM). A. Total RNA was extracted from OVCAR-3 cells. qRT-PCR determined the 17β-HSD7 mRNA level 72 h after siRNA transfection. Means and standard deviations are presented (n=3). B. Data reported as % of DNA synthesis *vs*. hormone-free control (100%). After treatment with siRNA for 96 h, 17β-HSD7 siRNA was compared with control siRNA in OVCAR-3 cells. C. 17β-HSD7 siRNA was compared with control siRNA in SKOV-3 cells. D. Cell cycle was analyzed by flow cytometry with DAPI/Triton X-100 solution. 17β-HSD7 siRNA was compared with control siRNA in OVCAR-3 cells. E. 17β-HSD7 siRNA was compared with control siRNA in SKOV-3 cells. Data are shown as the percentage of total cells in G0/G1, S, and G2/M phase. Quadruple wells were used for each condition and repeated in three independent experiments. Error bars represent SD. $^{*}P\leq0.05$ *vs*. control; $^{**}P\leq0.001$ *vs*. control by Student's test.

In 17β-HSD7 knocked down SKOV-3 cells, there were significant proliferation decreases with siRNA vs. control, at 28% in the presence of 0.1 nM E1, 25% with 100 nM DHEA and 29% with 1 μM DHEA (**Figure 2C**). In 17β-HSD7 knocked down OVCAR-3 cells, there was a significant decrease in cell proliferation (18%) compared with control siRNA, in the presence of 0.1 nM E1 (**Figure 2B**). Thus, knockdown of 17β-HSD7 significantly inhibited EOC cell growth. Cell proliferation decreased (by 21-25%) following transfection with 17β-HSD1 siRNA in the presence of either substrate in OVCAR-3 cells (**Figure 4B**). In SKOV-3 cells, cell proliferation decreased by 12% following transfection of 17β-HSD1 siRNA only in the presence of 100 nM DHEA (**Figure 4C**).

The flow cytometry assay was carried out to compare the direct impact of different hormones on EOC cells after transfection with siRNAs. The decreased expression of 17β-HSD7 produced an arrest of the cell cycle in the G2/M phase. In OVCAR-3 cells, the cell arrest in G2/M increased by 20% with 0.1 nM E1, 26% with 1 μM DHEA (**Figure 2D**), and 17% with 100 nM DHEA. Cell arrest in G2/M increased by 25% with 0.1 nM E1 in SKOV-3 cells (**Figure 2E**). 17β-HSD7 knockdown induced cell cycle arrest concomitant with the modulation of cell cycle protein cyclin B1/Cdk1. Western blot analysis confirmed this in both cell lines.

The expression of cyclin B1 in OVCAR-3 decreased 20% (CV: 2%) with 1 μM DHEA and 27% (CV: 10%) with 100 nM DHEA (**Figure 3A**) with siRNA treatment. In SKOV-3 cells cyclin B1 expression significant decreased 20% (CV: 2%) with 0.1 nM E1, 39% (CV: 3%) with 1 μM DHEA, 37% (CV: 4%) with 100 nM DHEA vs. control (**Figure 3B**). The knockdown of 17β-HSD7 significantly suppressed expression of Cdk1 compared with the control -19% (CV: 5%) with 0.1 nM E1, -20% (CV: 3%) with 1 μM DHEA in OVCAR-3 (**Figure 3A**). In SKOV-3 cells, the expression of Cdk1 was also significantly knocked down -16% (CV: 2%) with 0.1 nM E1, -27% (CV: 13%) (100 nM DHEA) vs. control (**Figure 3B**). The results demonstrated that the knockdown of 17β-HSD7 arrested cell cycle in the G2/M phase together with the downregulation of the cyclin B1/Cdk1 complex.

Reductive 17β-HSD knockdown blocked E2 formation and DHT degradation

In SKOV-3 cells (**Table 3**), 17β-HSD7 knockdown significantly blocked E2 formation and restored DHT concentration. 17β-HSD7 knockdown decreased the E2 level by 60%, induced a 34%-increase in DHT in the presence of 1 μM DHEA and decreased the E2 level by 68% in the presence of 100 nM DHEA. Furthermore, following provision of 1 μM DHEA as substrate, the E2 level dropped 35%, and the DHT level increased 11% in 17β-HSD1 knocked down cells. In OVCAR-3 cells (**Table 3**), 17β-HSD1 knockdown displayed a significant effect on the reduction of the E2 level and restoration of the DHT concentration. The E2 level decreased 65% in the presence of 100 nM DHEA and 89% in the presence of 1 μM DHEA. The DHT concentration increased to 142% in the presence of 1 μM DHEA.

Inhibitors of reductive 17β-HSDs suppressed cell proliferation

The selective inhibitor INH7(81) [30] or the 17β-HSD1 inhibitor INH1(18) [29] exhibited specific inhibitory potency on the conversion of E1 into E2, with relative IC_{50} in **Table 1**. To investigate the anti-proliferative effect of INH7(81) a concentration of 4 μM ($10\times IC_{50}$) was used. From the results of previous studies a concentration of 2 μM ($10\times IC_{50}$) INH1(18) was used [19, 29]. The results were similar to that from the 17β-HSD7 knockdown.

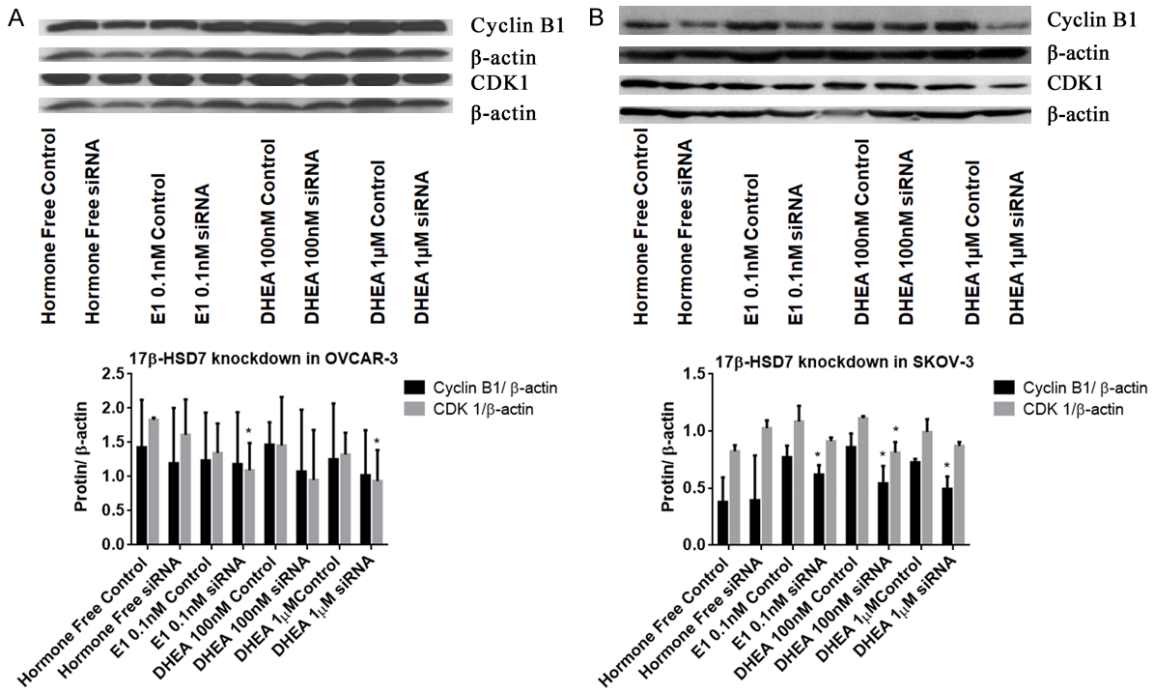

Figure 3. 17β-HSD7 knockdown-induced cell cycle arrest was concomitant with cyclin B1/Cdk1 expression modulation. Total protein was extracted from EOC cells. 100 nM mixed 17β-HSD7-specific siRNA and control siRNA were used. Western blot analysis determined cyclin B1 expression after 96 h after siRNA transfection. Anti-cyclin B1 antibody was used to reveal bands at molecular weight 58 kDa, anti-β-actin identified bands at molecular weight 42 kDa. Each experiment was repeated in three independent experiments. Error bars represent SD. *P≤0.05 *vs.* control; **P≤0.001 *vs.* control by Student's test.

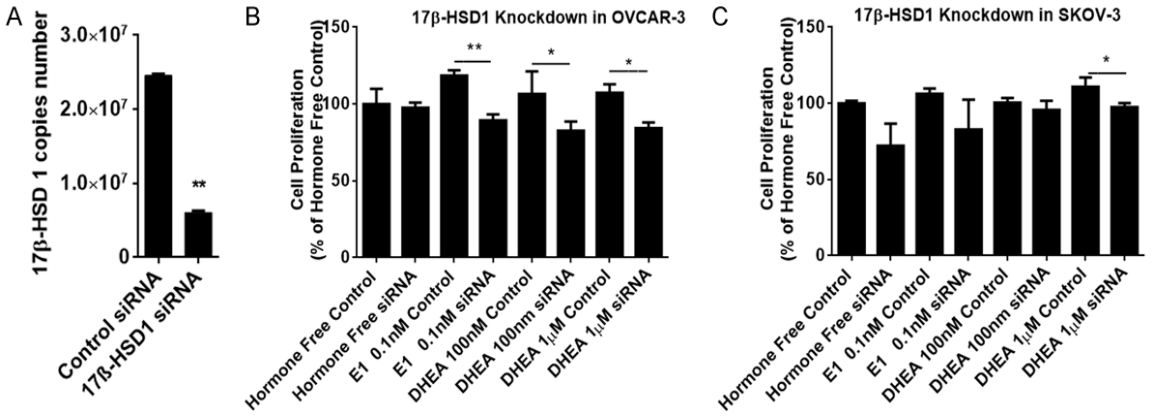

Figure 4. Cell proliferation after 17β-HSD1 siRNA transfection 96 h in EOC cells. 100 nM mixed 17β-HSD1-specific siRNA and control siRNA were used. Different hormone sources were provided: E1 (0.1 nM) and DHEA (100 nM and 1 μM). A. Total RNA was extracted from OVCAR-3 cells. qRT-PCR determined the 17β-HSD1 mRNA level 72 h after siRNA transfection. Means and standard deviations are presented (n=3). B. Data are reported as % of DNA synthesis *vs.* hormone-free control (100%). 17β-HSD1 siRNA was compared with control siRNA in OVCAR-3 cells. C. 17β-HSD1 siRNA was compared with control siRNA in SKOV-3 cells. Quadruple wells were used for each condition and repeated in three independent experiments. Error bars represent SD. *P≤0.05 *vs.* control; **P≤0.001 *vs.* control by Student's test.

After 144-hour treatment with INH7(81), OVCAR-3 cell proliferation decreased by 32% in the presence of 0.1 nM E1 and 20% with 100 nM DHEA shown in **Figure 5A** and **5B**. In SKOV-3 cells, there was a significant decrease in cell proliferation in the INH7(81)-treated

Table 3. Knockdown 17β-HSD1 or 17β-HSD7 blocked E2 formation and DHT degradation

	OVCAR-3 E2 (pM)	OVCAR-3 DHT (pM)	SKOV-3 E2 (pM)	SKOV-3 DHT (pM)
Hormone Free Control	0.009±0.0008	0.305±0.012	0.049±0.001	0.380±0.039
E1 0.1 nM Control	0.655±0.040	0.352±0.010	196.507±15.836	0.435±0.011
E1 0.1 nM HSD17B1 siRNA	0.215±0.026	0.647±0.079	143.457±16.227	0.530±0.019
E1 0.1 nM HSD17B7 siRNA	0.249±0.014	0.504±0.014	85.686±1.123	0.558±0.093
DHEA 100 nM Control	58.164±1.886	12.759±1.038	353.063±37.976	228.250±22.852
DHEA 100 nM HSD17B1 siRNA	20.326±1.879*	34.978±3.743	216.138±27.978	262.839±22.931
DHEA 100 nM HSD17B7 siRNA	36.562±0.484	30.279±2.546	142.615±9.692*	280.104±24.867
DHEA 1 μM Control	339.187±21.681	510.263±26.289	755.798±48.961	1627.624±120.428
DHEA 1 μM HSD17B1 siRNA	38.479±1.360*	726.201±48.910*	491.081±21.997*	1800.354±524.548*
DHEA 1 μM HSD17B7 siRNA	121.364±10.373	512.320±20.849	242.882±10.670*	2173.708±540.400*

Data represent the mean values ± SD of three independent experiments. *, P≤0.05 *vs.* control by Student's test.

group compared with the control (0.1 nM E1, 26%) as shown in **Figure 5E** and a 32% decrease with 100 nM DHEA in **Figure 5F**. In OVCAR-3 cells (**Figure 5D**), INH7(81) displayed a significant effect on the reduction of the E2 level and restoration of the DHT concentration. The E2 level decreased 56% in the presence of 0.1 nM E1 and 50% with 100 nM DHEA. DHT accumulation increased 22.7-fold in the presence of 0.1 nM E1 and 8.7-fold with 100 nM DHEA. In SKOV-3 cells (**Figure 5H**), INH7(81) also showed significant results. INH7(81) resulted in a 36% decrease in the E2 level in the presence of 0.1 nM E1 and a 62% decrease with 100 nM DHEA. The DHT level increased 37.8-fold in the presence of 0.1 nM E1 and 5.5-fold with 100 nM DHEA. These results demonstrate that the 17β-HSD7 inhibitor INH7(81) had strong efficacy on sex-hormone regulation in both EOC cell lines.

After treatment with INH1 inhibitor for 144 hours, cell proliferation showed a 14% decrease in OVCAR-3 cells in the presence of 0.1 nM E1 (**Figure 5A**) and 5% with 100 nM DHEA (**Figure 5B**). INH1(18) had a modest effect on SKOV-3 cell proliferation in the presence of 0.1 nM E1 or 100 nM DHEA (**Figure 5E** and **5F**). In OVCAR-3 cells (**Figure 5C**), INH1(18) produced a significant decrease in E2 level (24%) in the presence of 1 μM DHEA. In SKOV-3 cells (**Figure 5G**), INH1(18) displayed a similar potency in the presence of 0.1 nM E1, whereas it induced the accumulation of DHT by 1.8-fold. These results show that the 17β-HSD7 inhibitor INH7(81) had a stronger effect on EOC cell growth than INH1(18), an inhibitor of 17β-HSD1.

Contribution of additional DHT on EOC cell proliferation dependent on E2

To evaluate the impact of DHT on EOC, DHT ranging from 0.01 nM to 10 nM was added to test its effect on E2 stimulated EOC cell growth. The cells in the culture media were treated with HF medium with 0.1 nM E2. Results showed that the addition of DHT decreased EOC cell proliferation. Both DHT concentrations 0.5 nM and 10 nM decreased similarly (10%) in OVCAR-3 (**Figure 6A**). In our experiment, the DHT concentration ranging from 0.5 nM to 2 nM significantly inhibited E2 stimulated SKOV-3 cell growth by 17% to 21% (**Figure 6C**). The inhibition effect decreased with high additional concentration at 5 nM and 10 nM of DHT (9% to 4%). We evaluated a correlation between 17β-HSD1 and the decreasing effect of DHT on EOC cell growth. Both EOC cell lines were treated with 2 μM INH1(18) for six days in the presence of 0.1 nM E1. The DHT addition decreased the cell proliferation of 17β-HSD1 inhibited cells. The cell proliferation decreased, followed by increasing DHT concertation in OVCAR-3 with 17β-HSD1 inhibition (**Figure 6B**). Its cell proliferation decreased 9%, supplemented with 10 nM DHT compared to the INH1 control group. The SKOV-3 cell proliferation significantly decreased from 10% to 22% supplemented with 0.01 nM to 2 nM DHT addition vs. INH1 control (**Figure 6D**). The decreases were only 15% and 13%, with higher concentration 5 nM and 10 nM DHT. DHT can

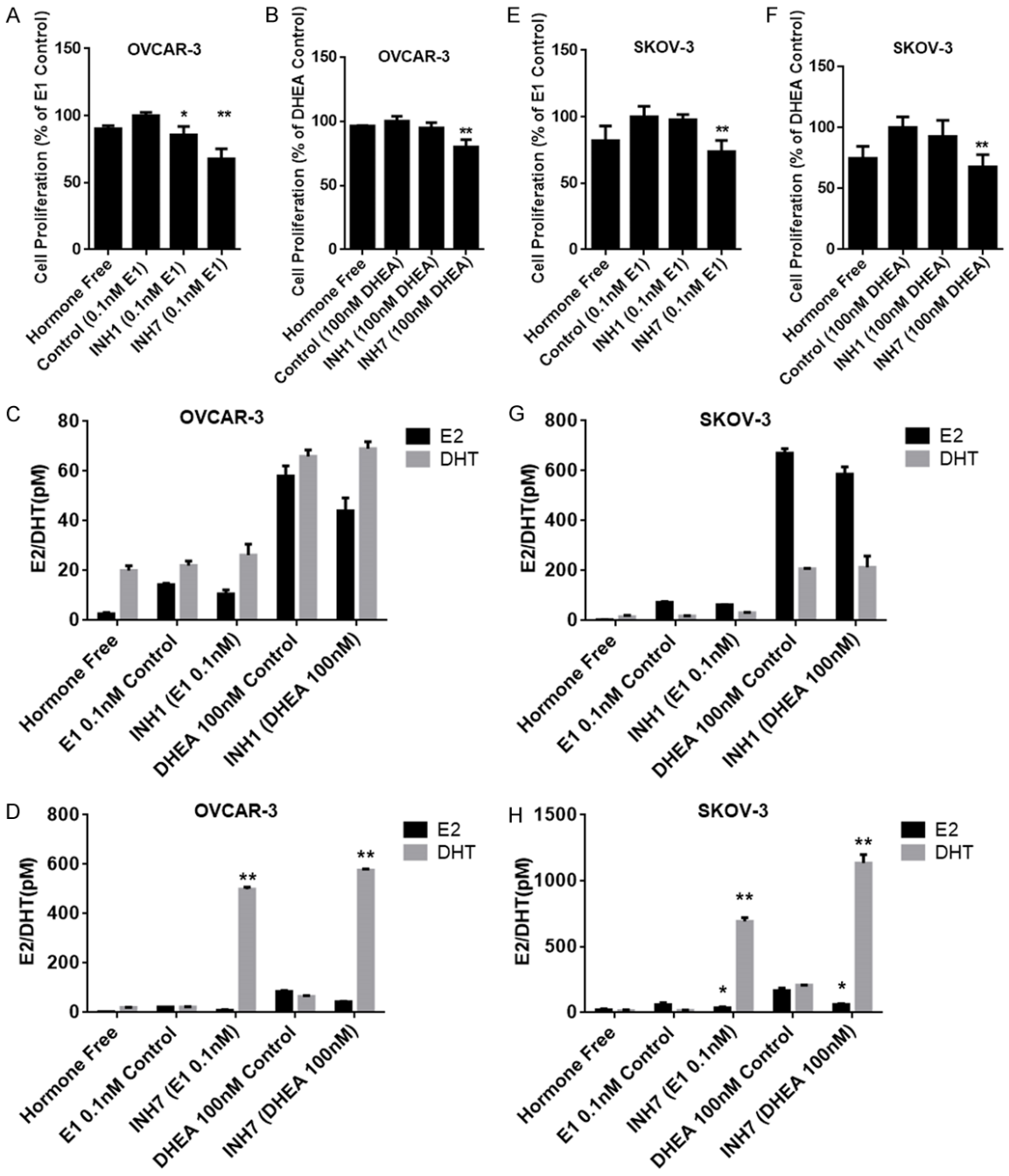

Figure 5. The inhibitors' effect in EOC cells. Cells were treated with inhibitors for 144 hours in the presence of substrates. A. Cell proliferation in OVCAR-3 cells with 0.1 nM E1. B. Cell proliferation in OVCAR-3 cells with 100 nM DHEA. C. E2/DHT concentration in OVCAR-3 cells after treatment with INH1. D. E2/DHT concentration in OVCAR-3 cells after treatment with INH81. E. Cell proliferation in SKOV-3 cells in the presence of 0.1 nM E1. F. Cell proliferation in SKOV-3 cells in the presence of 100 nM DHEA. G. E2/DHT concentration in SKOV-3 cells after treatment with INH1. H. E2/DHT concentration in SKOV-3 cells after treatment with INH81. Cell proliferation data reported as % of DNA synthesis *vs*. hormone-free control (100%). Quadruple wells were used for each condition and repeated in three independent experiments. Error bars represent SD. $^{*}P\leq0.05$ *vs*. control; $^{**}P\leq0.001$ *vs*. control by Student's test.

inhibit E2-stimulated growth in EOC cells and 17β-HSD1 inhibited EOC cell growth, especially when the additional DHT concentration ranging from 0.5 nM to 2 nM.

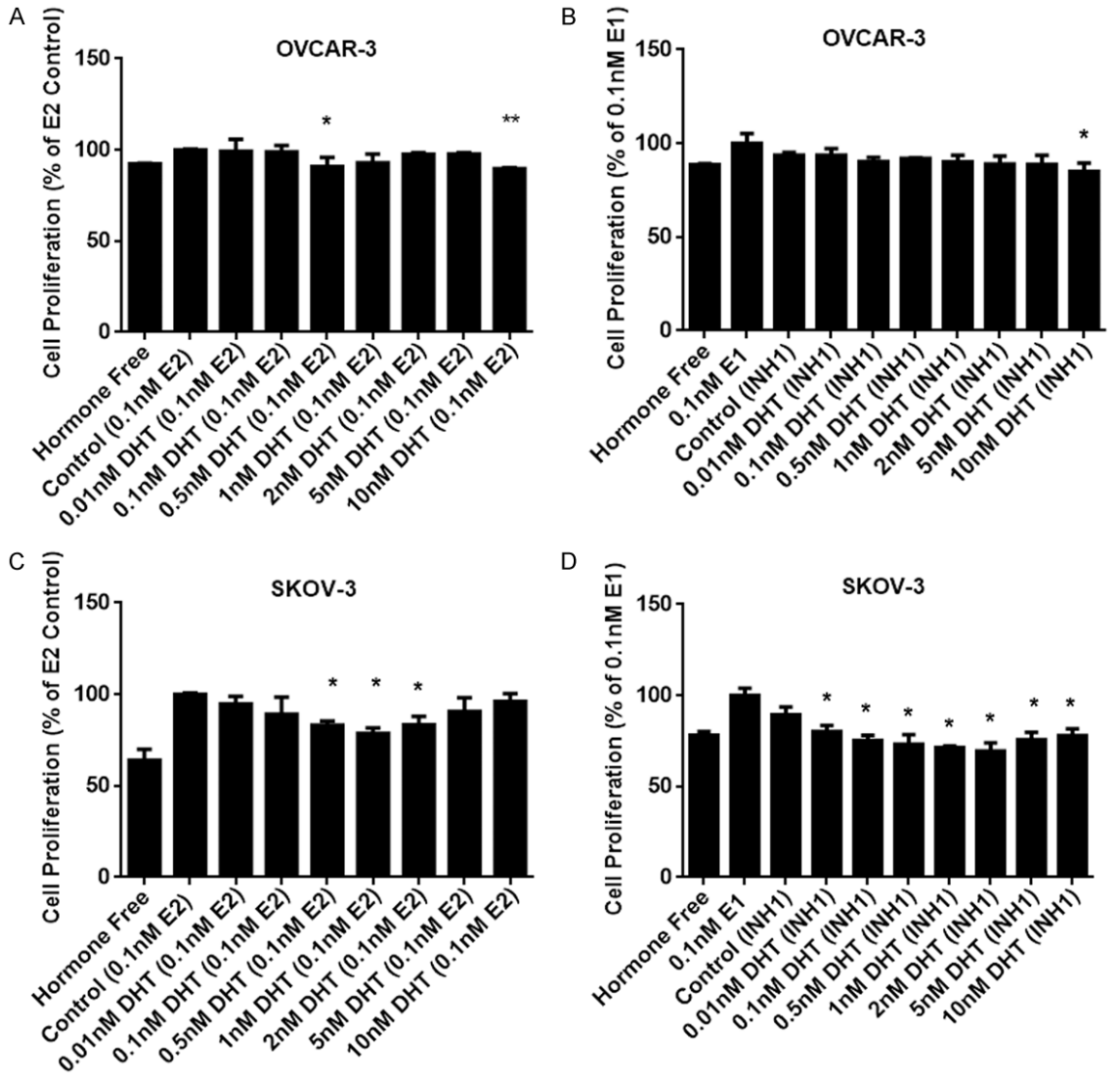

Figure 6. Contribution of E2 and DHT on EOC cell proliferation. Cells were treated with DHT in the range of 0.01 nM to 10 nM DHT for 6 days. A. Cell proliferation in OVCAR-3 cells supplemented with 0.1 nM E2. B. Cell proliferation in OVCAR-3 cells with 2 μM INH1 in the presence of 0.1 nM E1. C. Cell proliferation in SKOV-3 cells supplemented with 0.1 nM E2. D. Cell proliferation in SKOV-3 cells with 2 μM INH1 in the presence of 0.1 nM E1. Cell proliferation data reported as % of DNA synthesis *vs*. control (100%). Quadruple wells were used for each condition and repeated in three independent experiments. Error bars represent SD. $^{*}P\leq0.05$ *vs*. control; $^{**}P\leq0.001$ *vs*. control by Student's test.

Discussion

The development of new treatments and improvement of early detection are research priorities for EOC. Both estrogens and androgens are of critical importance in the study of EOC [28]. Estrogens induce ovarian cancer epithelial-mesenchymal transition (EMT) [5], an important stage of cancer metastasis whereby epithelial cells lose cellular adhesion and cell polarity, acquire motility and aggressiveness to become mesenchymal cells [29]. Activation of EMT is related to chemoresistance, and it causes cancer recurrence and metastasis after chemotherapy and radiation treatments [30, 31]. Most women diagnosed with advanced EOC will present with recurrence within 18 months that typically evolves to chemotherapy resistance [6]. The selective ER modulator tamoxifen competitively inhibits ER, blocking its downstream signaling to generate anti-estrogenic effects. Tamoxifen has been tested

in OC phase II clinical trials, and the trial results showed a modest response rate [11]. As mentioned above, the majority of OC cases are diagnosed during postmenopausal years. Aromatase inhibitors (AI) such as letrozole and anastrozole block the production of estrogens and have been investigated for the treatment of recurrent or persistent OC [32]. They have been tested in a select group of ER+ patients achieving a partial objective response rate 0-11% [11]. Androgens stimulate the expression, activity, and phosphorylation of telomerase in OC cells [14]. The most potent androgen, DHT, shows an inhibitory effect on the expression of transforming growth factor beta 1 (TGF-β1) receptors (TGFBR1-TGFBR2) in EOC cells, which may cause a disorder in the TGF-β1 response and the cyclin-dependent kinase inhibitor p21 downregulation [33, 34]. In clinical trials on recurrent cancers, antiandrogenic compounds have been used in OC management. The treatment includes gonadotropin-releasing hormone (goserelin, triptorelin, and leuprolide) and AR antagonists (bicalutamide and flutamide) [35]. The novel CYP17 inhibitor abiraterone, which blocks the generation of adrenal steroids downstream of CYP17, was also evaluated in clinical trials [36]. Nevertheless clinical trials involving endocrine therapy have yielded mixed results [20]. The correlative effect between E2 and DHT on EOC growth remained to be understood before our study.

The reductive 17β-HSDs are expressed in human ovarian surface epithelium [37]. Steroidogenesis data showed that 17β-HSDs are still active in postmenopausal ovaries, and that these enzymes' function decreased with time after menopause [21, 38]. 17β-HSD2 and 17β-HSD5 were detected in EOC tissue at lower mRNA expression levels compared with normal human surface epithelium, but data is still limited concerning reductive 17β-HSD1 and 7 expression in EOC cells and tissue [28].

We demonstrated that 17β-HSD7 is expressed in the tissue from serous ovarian adenocarcinoma, the most common subtype of EOC in clinical data analysis. We found that the expression of 17β-HSD7 is significantly upregulated in EOC tissue compared with the normal ovary. 17β-HSD7 has also a significant upregulation (2.50-fold, $P<0.0001$) in hormone-responsive breast tumor [39]. Furthermore, its expression in EOC cell lines OVCAR-3 and SKOV-3 was confirmed. OVCAR-3 cells are positive for estrogen, androgen, and progesterone receptors, which is useful for investigating sex hormone-converting enzymes in EOC [40]. SKOV-3 cells show resistance to several cytotoxic drugs and tumor necrosis factors. 17β-HSD7 is expressed more in SKOV-3 than in OVCAR-3 cells, and its corresponding mRNA level is almost twice that in OVCAR-3. The other important reductive enzyme, 17β-HSD1 is expressed in both EOC cells OVCAR-3 and SKOV-3.

Reductive 17β-HSD7 is a dual intracrine regulator: it regulates the most potent estrogen E2 and the most active androgen DHT [16]. On the contrary, 17β-HSD1 is more specific toward estrogen [41]. Enzyme kinetics and X-ray crystallographic studies found that type 1 also inactivates the most active androgen DHT, but the androgen activity is significantly less than 17β-HSD7 [42]. A recent study showed that androgens act as antiproliferative agents in the presence of estrogens in hormone-dependent BC [43-45]. An *in vivo* study of estrogen-dependent BC found that specific inhibition of 17β-HSD7 can lead to shrinkage of the tumor with decreased E2 and increased DHT levels in plasma [16]. The inhibitors of 17β-HSD7 demonstrated significant effects in the hormone-dependent BC: INH7(80) reduced cell proliferation by 27.8% in MCF7 cells and 25.4% in T47D cells in the presence of 0.5 nM E1-S under the experimental conditions [44].

DHEA is the unique source of steroid hormones in post-menopausal women [46-48]. In our study, we used the upstream hormone DHEA as a steroid source to mimic the postmenopausal condition in ovarian cancer cell culture. We found that knocking down or inhibiting 17β-HSD7 significantly inhibited cell growth and arrested the cell cycle in the G2/M phase by inhibiting cyclin B1/Cdk1. The deficiency of the G2/M arrest checkpoint could allow the damaged cell to enter mitosis and go through apoptosis. Efforts to raise the effect could increase the cytotoxicity of chemotherapy toward cancer cells [49]. The cyclin B1/Cdk1 complex specifically regulates cell entry into mitosis [50]. Down-regulation of 17β-HSD7 affects the steroid pathways between E1 and E2 and 3β-diol and DHT in cells. Knockdown of 17β-HSD7 blocked E2 formation and DHT degradation, suppressing EOC growth. 17β-HSD1

also plays roles in regulating E2, the most potent estrogen, synthesized from E1 and has a role in the conversion of 4-dione to testosterone [51]. Down-regulation of 17β-HSD1 affects the steroid pathway between E1 and E2 in cells, resulting in decrease of intercellular E2 levels. But the effect of down-regulating 17β-HSD1 on EOC grown and the cell cycle is not so significant as that of 17β-HSD7.

We tested inhibitors INH7(81) and INH1(18) in EOC cells and achieved similar results to the effects of siRNAs in OVCAR-3 and SKOV-3 cells. The two inhibitors decreased cell proliferation and led to lower E2 and higher DHT levels in both cell lines. The INH7(81) has stronger effect on cell proliferation and steroid concentration regulation. Our study demonstrated that DHT has an anti-proliferation effect on EOC cells growth in the presence of estrogens, especially at the low concentration. DHT has a similar role in EOC as in hormone-dependent BC. The knock-down of 17β-HSD1 can have a stronger influence on EOC with additional low concertation DHT.

17β-HSD7 is well known to possess a significant effect in sex hormone control [16, 22]. Its overexpression in EOC tissues and its impact on EOC cell growth support the importance of sex hormones in EOC development, similar to the hormone-dependent BC in this respect. The over-expression and effect of the important sex-hormone converting dehydrogenase 17β-HSD7 in both BC and EOC support the sex-hormone association for these cancers.

We demonstrated that the 17β-HSD7 inhibitor can play protective effects against EOC cell proliferation by inhibiting its dual effects regulating E2 and DHT in cell levels, as in the hormone-dependent BC [16, 44]. Thus, the over-expression of 17β-HSD7 in EOC provides a novel potential diagnostic biomarker for EOC. Treatment involving joint targeting of E2 synthesis and DHT degradation is a new concept for EOC. From the present results, it is evident that targeting 17β-HSD7 can open a new avenue for EOC treatment that can be critical for the fight against this deadly disease.

Acknowledgements

RX. Wang was supported by the UL/Chinese Scholarship Committee joint scholarship. We thank Dr. Donald Poirier for providing us with INH1(18). We would also like to thank Dr. Muriel Kelly for English editing.

Disclosure of conflict of interest

None.

Address correspondence to: Sheng-Xiang Lin, Axe Molecular Endocrinology and Nephrology, CHU Research Center and Université Laval, 2705 Boulevard Laurier, Sainte-Foy, Québec G1V 4G2, Canada. Tel: 418-654-2296; Fax: 418-654-2761; E-mail: sheng-xiang.lin@crchudequebec.ulaval.ca

References

[1] Siegel R, Naishadham D and Jemal A. Cancer statistics, 2013. CA Cancer J Clin 2013; 63: 11-30.
[2] Torre LA, Trabert B, DeSantis CE, Miller KD, Samimi G, Runowicz CD, Gaudet MM, Jemal A and Siegel RL. Ovarian cancer statistics, 2018. CA Cancer J Clin 2018; 68: 284-296.
[3] Cho KR and Shih Ie M. Ovarian cancer. Annu Rev Pathol 2009; 4: 287-313.
[4] Cannistra SA. Cancer of the ovary. N Engl J Med 2004; 351: 2519-2529.
[5] Jeon SY, Hwang KA and Choi KC. Effect of steroid hormones, estrogen and progesterone, on epithelial mesenchymal transition in ovarian cancer development. J Steroid Biochem Mol Biol 2016; 158: 1-8.
[6] Jayson GC, Kohn EC, Kitchener HC and Ledermann JA. Ovarian cancer. Lancet 2014; 384: 1376-1388.
[7] Powless CA, Aletti GD, Bakkum-Gamez JN and Cliby WA. Risk factors for lymph node metastasis in apparent early-stage epithelial ovarian cancer: implications for surgical staging. Gynecol Oncol 2011; 122: 536-540.
[8] Colombo N, Guthrie D, Chiari S, Parmar M, Qian W, Swart AM, Torri V, Williams C, Lissoni A and Bonazzi C; International Collaborative Ovarian Neoplasm (ICON) collaborators. International Collaborative Ovarian Neoplasm trial 1: a randomized trial of adjuvant chemotherapy in women with early-stage ovarian cancer. J Natl Cancer Inst 2003; 95: 125-132.
[9] Trimbos B, Timmers P, Pecorelli S, Coens C, Ven K, Van Der Burg M and Casado A. Surgical staging and treatment of early ovarian cancer: long-term analysis from a randomized trial. J Natl Cancer Inst 2010; 102: 982-987.
[10] Lukanova A and Kaaks R. Endogenous hormones and ovarian cancer: epidemiology and current hypotheses. Cancer Epidemiol Biomarkers Prev 2005; 14: 98-107.

[11] Modugno F, Laskey R, Smith AL, Andersen CL, Haluska P and Oesterreich S. Hormone response in ovarian cancer: time to reconsider as a clinical target? Endocr Relat Cancer 2012; 19: R255-R279.
[12] Saad AF, Hu W and Sood AK. Microenvironment and pathogenesis of epithelial ovarian cancer. Horm Cancer 2010; 1: 277-290.
[13] Kuhnel R, de Graaff J, Rao BR and Stolk JG. Androgen receptor predominance in human ovarian carcinoma. J Steroid Biochem 1987; 26: 393-397.
[14] Nourbakhsh M, Golestani A, Zahrai M, Modarressi MH, Malekpour Z and Karami-Tehrani F. Androgens stimulate telomerase expression, activity and phosphorylation in ovarian adenocarcinoma cells. Mol Cell Endocrinol 2010; 330: 10-16.
[15] Labrie F, Luu-The V, Lin SX, Simard J, Labrie C, El-Alfy M, Pelletier G and Belanger A. Intracrinology: role of the family of 17 beta-hydroxysteroid dehydrogenases in human physiology and disease. J Mol Endocrinol 2000; 25: 1-16.
[16] Wang X, Gerard C, Theriault JF, Poirier D, Doillon CJ and Lin SX. Synergistic control of sex hormones by 17beta-HSD type 7: a novel target for estrogen-dependent breast cancer. J Mol Cell Biol 2015; 7: 568-579.
[17] Xu D, Aka JA, Wang R and Lin SX. 17beta-hydroxysteroid dehydrogenase type 5 is negatively correlated to apoptosis inhibitor GRP78 and tumor-secreted protein PGK1, and modulates breast cancer cell viability and proliferation. J Steroid Biochem Mol Biol 2017; 171: 270-280.
[18] Bowman A, Gabra H, Langdon SP, Lessells A, Stewart M, Young A and Smyth JF. CA125 response is associated with estrogen receptor expression in a phase II trial of letrozole in ovarian cancer: identification of an endocrine-sensitive subgroup. Clin Cancer Res 2002; 8: 2233-2239.
[19] Smyth JF, Gourley C, Walker G, MacKean MJ, Stevenson A, Williams AR, Nafussi AA, Rye T, Rye R, Stewart M, McCurdy J, Mano M, Reed N, McMahon T, Vasey P, Gabra H and Langdon SP. Antiestrogen therapy is active in selected ovarian cancer cases: the use of letrozole in estrogen receptor-positive patients. Clin Cancer Res 2007; 13: 3617-3622.
[20] Chura JC, Ryu HS, Simard M, Poirier D, Tremblay Y, Brooker DC, Blomquist CH and Argenta PA. Steroid-converting enzymes in human ovarian carcinomas. Mol Cell Endocrinol 2009; 301: 51-58.
[21] Havelock JC, Rainey WE, Bradshaw KD and Carr BR. The post-menopausal ovary displays a unique pattern of steroidogenic enzyme expression. Hum Reprod 2006; 21: 309-317.
[22] Zhang CY, Wang WQ, Chen J and Lin SX. Reductive 17beta-hydroxysteroid dehydrogenases which synthesize estradiol and inactivate dihydrotestosterone constitute major and concerted players in ER+ breast cancer cells. J Steroid Biochem Mol Biol 2015; 150: 24-34.
[23] Wang XQ, Aka JA, Li T, Xu D, Doillon CJ and Lin SX. Inhibition of 17beta-hydroxysteroid dehydrogenase type 7 modulates breast cancer protein profile and enhances apoptosis by down-regulating GRP78. J Steroid Biochem Mol Biol 2017; 172: 188-197.
[24] Xu D and Lin SX. Mimicking postmenopausal steroid metabolism in breast cancer cell culture: differences in response to DHEA or other steroids as hormone sources. J Steroid Biochem Mol Biol 2016; 161: 92-100.
[25] Blomquist CH, Bonenfant M, McGinley DM, Posalaky Z, Lakatua DJ, Tuli-Puri S, Bealka DG and Tremblay Y. Androgenic and estrogenic 17β-hydroxysteroid dehydrogenase/17-ketosteroid reductase in human ovarian epithelial tumors: evidence for the type 1, 2 and 5 isoforms. J Steroid Biochem Mol Biol 2002; 81: 343-351.
[26] Laplante Y, Cadot C, Fournier MA and Poirier D. Estradiol and estrone C-16 derivatives as inhibitors of type 1 17β-hydroxysteroid dehydrogenase: blocking of ER+ breast cancer cell proliferation induced by estrone. Bioorg Med Chem 2008; 16: 1849-1860.
[27] Bellavance É, Luu-The V and Poirier D. Potent and selective steroidal inhibitors of 17β-hydroxysteroid dehydrogenase type 7, an enzyme that catalyzes the reduction of the key hormones estrone and dihydrotestosterone. J Med Chem 2009; 52: 7488-7502.
[28] Ren X, Wu X, Hillier SG, Fegan KS, Critchley HO, Mason JI, Sarvi S and Harlow CR. Local estrogen metabolism in epithelial ovarian cancer suggests novel targets for therapy. J Steroid Biochem Mol Biol 2015; 150: 54-63.
[29] Larue L and Bellacosa A. Epithelial-mesenchymal transition in development and cancer: role of phosphatidylinositol 3' kinase/AKT pathways. Oncogene 2005; 24: 7443-7454.
[30] Iwatsuki M, Mimori K, Yokobori T, Ishi H, Beppu T, Nakamori S, Baba H and Mori M. Epithelial-mesenchymal transition in cancer development and its clinical significance. Cancer Sci 2010; 101: 293-299.
[31] Abdullah LN and Chow EK. Mechanisms of chemoresistance in cancer stem cells. Clin Transl Med 2013; 2: 3.
[32] Cunat S, Rabenoelina F, Daures JP, Katsaros D, Sasano H, Miller WR, Maudelonde T and Pujol P. Aromatase expression in ovarian epithelial cancers. J Steroid Biochem Mol Biol 2005; 93: 15-24.
[33] Kohan-Ivani K, Gabler F, Selman A, Vega M and Romero C. Role of dihydrotestosterone (DHT) on TGF-beta1 signaling pathway in epithelial

ovarian cancer cells. J Cancer Res Clin Oncol 2016; 142: 47-58.
[34] Alsina-Sanchis E, Figueras A, Lahiguera A, Gil-Martin M, Pardo B, Piulats JM, Marti L, Ponce J, Matias-Guiu X, Vidal A, Villanueva A and Vinals F. TGFbeta controls ovarian cancer cell proliferation. Int J Mol Sci 2017; 18: 1658.
[35] Papadatos-Pastos D, Dedes KJ, de Bono JS and Kaye SB. Revisiting the role of antiandrogen strategies in ovarian cancer. Oncologist 2011; 16: 1413-1421.
[36] Barrie SE, Potter GA, Goddard PM, Haynes BP, Dowsett M and Jarman M. Pharmacology of novel steroidal inhibitors of cytochrome P450(17) alpha (17 alpha-hydroxylase/C17-20 lyase). J Steroid Biochem Mol Biol 1994; 50: 267-273.
[37] Rae MT and Hillier SG. Steroid signalling in the ovarian surface epithelium. Trends Endocrinol Metab 2005; 16: 327-333.
[38] Brodowska A, Brodowski J, Laszczyńska M, Słuczanowska-Głąbowska S, Rumianowski B, Rotter I, Starczewski A and Ratajczak MZ. Immunoexpression of aromatase cytochrome P450 and 17β-hydroxysteroid dehydrogenase in women's ovaries after menopause. J Ovarian Res 2014; 7: 52.
[39] Li T, Zhang W and Lin SX. Steroid enzyme and receptor expression and regulations in breast tumor samples-a statistical evaluation of public data. J Steroid Biochem Mol Biol 2020; 196: 105494.
[40] Ho SM. Estrogen, progesterone and epithelial ovarian cancer. Reprod Biol Endocrinol 2003; 1: 73.
[41] Theriault JF and Lin SX. The dual sex hormone specificity for human reductive 17beta-hydroxysteroid dehydrogenase type 7: synergistic function in estrogen and androgen control. J Steroid Biochem Mol Biol 2019; 186: 61-65.
[42] He W, Gauri M, Li T, Wang R and Lin SX. Current knowledge of the multifunctional 17β-hydroxysteroid dehydrogenase type 1 (HSD17B1). Gene 2016; 588: 54-61.
[43] Nicolás Díaz-Chico B, Germán Rodríguez F, González A, Ramírez R, Bilbao C, Cabrera De León A, Aguirre Jaime A, Chirino R, Navarro D and Díaz-Chico JC. Androgens and androgen receptors in breast cancer. J Steroid Biochem Mol Biol 2007; 105: 1-15.
[44] Sang X, Han H, Poirier D and Lin SX. Steroid sulfatase inhibition success and limitation in breast cancer clinical assays: an underlying mechanism. J Steroid Biochem Mol Biol 2018; 183: 80-93.
[45] Aka JA, Mazumdar M, Chen CQ, Poirier D and Lin SX. 17β-hydroxysteroid dehydrogenase type 1 stimulates breast cancer by dihydrotestosterone inactivation in addition to estradiol production. Mol Endocrinol 2010; 24: 832-845.
[46] Labrie F. All sex steroids are made intracellularly in peripheral tissues by the mechanisms of intracrinology after menopause. J Steroid Biochem Mol Biol 2015; 145: 133-138.
[47] Judd HL, Judd GE, Lucas WE and Yen SS. Endocrine function of the postmenopausal ovary: concentration of androgens and estrogens in ovarian and peripheral vein blood. J Clin Endocrinol Metab 1974; 39: 1020-1024.
[48] Labrie F, Martel C and Balser J. Wide distribution of the serum dehydroepiandrosterone and sex steroid levels in postmenopausal women: role of the ovary? Menopause 2011; 18: 30-43.
[49] DiPaola RS. To arrest or not to G2-M cell-cycle arrest. Clin Cancer Res 2002; 8: 3311-3314.
[50] Wang Z, Fan M, Candas D, Zhang TQ, Qin L, Eldridge A, Wachsmann-Hogiu S, Ahmed KM, Chromy BA, Nantajit D, Duru N, He F, Chen M, Finkel T, Weinstein LS and Li JJ. Cyclin B1/Cdk1 coordinates mitochondrial respiration for cell-cycle G2/M progression. Dev Cell 2014; 29: 217-232.
[51] Lukacik P, Kavanagh KL and Oppermann U. Structure and function of human 17β-hydroxysteroid dehydrogenases. Mol Cell Endocrinol 2006; 248: 61-71.

Supplementary Table 1. Sequences of 17β-HSD1, 7 and 5 specific siRNAs

	siRNA	Sense sequence (5' to 3')	Anti-sense sequence (5' to 3')
17β-HSD1	siRNA 1	GCUGGACGUGAAUGUAGUA	UACUACAUUCACGUCCAGC
	siRNA 2	GCCUUUCAAUGACGUUUAU	AUAAACGUCAUUGAAAGGC
	siRNA 3	CCACAGCAAGCAAGUCUUU	AAAGACUUGCUUGCUGUGG
17β-HSD7	siRNA 1	GGUACAGCAUUGACCAAUUTT	AAUUGGUCAAUGCUGUACCTG
	siRNA 2	GCAGGGUCUCUAUUCCAAUTT	AUUGGAAUAGAGACCCUGCTG
NC		UUCUCCGAACGUGUCACGUTT	ACGUGACACGUUCGGAGAATT